JOURNAL OF Applied Polymer SCIENCE

Effect of Organoclay and Silane Grafting of Polyethylene on Morphology, Barrierity, and Rheological Properties of HDPE/PA6 Blends

Ali Sharif-Pakdaman, Jalil Morshedian, Yousef Jahani
Department of Polymer Processing, Iran Polymer and Petrochemical Institute (IPPI), 14965/115 Tehran, Iran

Correspondence to: J. Morshedian (E-mail: j.morshedian@ippi.ac.ir)

ABSTRACT: Silane-grafted high-density polyethylene (HDPE-*g*-Si) was prepared by reactive extrusion. The grafted polyethylene (PE) was then melt compounded with organically modified montmorillonite and polyamide-6 (PA6) to form ternary nanocomposite. Fourier Transfer Infrared was used for investigation of grafting efficiency of specimens. Dispersion of clay in the blends and individual polymers were examined by X-ray diffraction (SAXS) and transmission electron microscopy (TEM). Scanning electron microscopy and dynamic rheology were also used for further study of microstructure along with compatibilization effect of silane grafting and adding organoclay in the blends. SAXS and TEM study showed that nanoclay was delaminated by PA6 or HDPE-*g*-Si chains, whereas the intercalation of neat HDPE in clay layers was negligible especially in higher level of clay. The morphological studies indicated that silane-grafted HDPE had hydrophilic characteristics and, therefore, was more compatible with PA6 than neat PE. Furthermore, in the same way adding nanoclay to this blends resulted in more uniform and finer morphology. And finally, results of oxygen and hydrocarbon permeability measurement demonstrated synergetic effect of silane grafting and presence of clay on barrierity improvement of samples. © 2012 Wiley Periodicals, Inc. J. Appl. Polym. Sci. 000: 000–000, 2012

KEYWORDS: compatibilization; morphology; blends; nanoparticles

Received 4 March 2012; accepted 24 April 2012; published online
DOI: 10.1002/app.37974

INTRODUCTION

Because of several advantages, polyethylene (PE) is probably the most widely used polymer in packaging applications. PE offers variety of advantages such as flexibility, light weight, low cost, and recyclability. However, the use of neat PE is restricted due to some of its inherent properties such as relatively poor barrier properties to oxygen and nonpolar materials which weakens long shelf life property required for these applications and make environmental and safety problems.[1–7]

In practice, a barrier function can be incorporated into PE packaging material with alternative technologies such as multilayer coextrusion (adding a layer of barrier material)[2] or blending of the base polymer with appropriate barrier materials.[2–8] Polyamide (PA), known for its outstanding hydrocarbon permeation barrier properties; in which, it often used as a blending component for PE because of advantages expected from good processability, relatively low price, and excellent physical and thermal properties.[4,6–9] Moreover, recently polymer–clay nanocomposite materials have attracted attention as an alternative route to improve polymer barrierity as well as other physical and mechanical properties of final products.[1–3,6,10] Parallel oriented plates-like impermeable particles (PA or clay particles) force penetrating gas molecules to wiggle around them in a random walk; hence, the gas diffuses by a tortuous pathway.[1]

In general, ultimate behaviors of polymer blends are highly dependent on the resulting morphology.[4–9] It is also recognized that superior properties of nanocomposites are attributed to the dispersion and orientation of clay layers as well as extensive delamination of layered clay structure. These desirable conditions attributed to suitable processing conditions and effective interaction between polymer matrix and dispersed phase.[1–10] In the case of PE, because of their nonpolar backbone, naturally polar PA and hydrophilic clay are immiscible with the polymer matrix. Consequently, modification of polymer molecules is highly required. The mostly used compatibilization method is introducing functionalized polymer containing polar groups, such as maleic anhydride-grafted or acrylic acid-grafted polymers as a compatibilizer, or using direct grafting or functionalizing reaction of polymer. It was claimed that these methods can effectively enhance the interfacial adhesion between the polymeric phases and also facilitates intercalation of polymer chain into clay galleries.[4,6–14]

Further studies were also done to show the effect of organoclay dispersion on morphology and other properties of PE-PA binary blends without or in presence of maleic anhydride or other compatibilizers.[6,15–21] The results obviously showed that the clay particles played the role of a coupling species between two polymers and increased the interaction of two phases in certain extent.

In a recent paper, we showed that silane grafting of high-density polyethylene (HDPE) chains successfully compatibilize them with montmorillonite nanoclay.[22] Another works[23,24] also explained that the alkoxy groups of silane used in manufacture of cross-linkable PE, which are mainly vinyl silane such as vinyltrimethoxysilane (VTMS), cause noticeable improvement of interfacial adhesion between PE and clay layers. However, the use of silane grafting of polyolefins in a blend with another polymer, was rarely published. Nachtigall et al.[25] reported the compatibilizing effect of using silane-grafted polypropylene (PP) in PP/PA6 blends. Another work also focused on effect of silane-grafted PP on morphology of PP/PA6/clay composites.[26]

The objective of this study is focused on synergetic effect of silane grafting of high-density polyethylene (HDPE-*g*-Si) and using organoclay on compatibilizing of HDPE/PA6/nanoclay ternary nanocomposites. For this goal, VTMS was used to graft on PE molecules in a reactive extrusion and prepared grafted polymer were then melt blended with PA6 with or without nanoclay. As a result, firstly we describe the effect of silane grafting of blow molding grade HDPE on compatibilization and morphology of HDPE-*g*-Si/PA6 blends. Then, effect of clay dispersion and delamination on prepared blends was investigated. Finally, barrier and rheological properties of these samples were elucidated.

EXPERIMENTAL

Materials

Commercial blow molding grade high-density polyethylene (HDPE, BL3) with MFI of 1.2 g/min (5 kg, 190°C) and density of 0.954 g/cm^3 was received from Jam petrochemical Company (Assaluyeh, Iran). Polyamide 6 (PA6, Ultramid® B40 01) was supplied from BASF Company (Freeport, Texas, USA); this polymer has a density of 1.13 g/cm^3 and viscosity number of 250 cm^3/g (0.5% in 96% sulfuric acid). Vinyltrimethoxysilane (VTMS) with commercial name of Dynasylan® Silfin-25 was purchased from Evonik (Essen, Germany). Dicumyl peroxide 99% (DCP) from Concord Company (Taipei, Taiwan) was used as an initiator. Calcium stearate from Merk Company was used as a processing aid in the melt compounding. Finally, Organo montmorinolite nanoclay (Org-MMT) modified with dimethyl, dehydrogenated tallow, quaternary ammonium salt (Cloisite® 15A) with density of 1.66 g/cm^3 and modifier concentration of 125 meq/100 g-clay was obtained from Rockwood Company (Gonzales, Texas, USA).

Sample Preparation

An appropriate amount of DCP was dissolved in VTMS. This solution was absorbed in PE granules during mixing in turbo mixer for about an hour in ambient temperature. From our previous researches,[22,27] and also try and error we set optimum amount of VTMS equal to 4 phr (weight part per hundred part of PE) and DCP equal to 0.1 phr for which best melt rheology and silane grafting efficiency was accessible. The enriched PE granules with VTMS and initiator then fed into corotating twin-screw extruder (Brabender, PLASTI-CORDER, Duisburg, Germany; with a length-to-diameter of 45) where grafting reaction was done. The maximum screw speed was 75 rpm and average residence time measured about 2 min. The prepared HDPE-*g*-Si or neat PE was then mixed with considered amount of PA and/or organoclay (the compositions of samples are reported in Table I) and again melt compounded in mentioned extruder with screw speed of 90 rpm. The PA6 was dried at 90°C during 16 h before blending. The residence time of mixing was kept constant in 2 min by reducing feeding into extruder. Temperature profile for grafting extrusion steps was (145, 160, 170, 180, 185, and 190°C) and for formulations consist of PA6 was (190, 205, 200, 220, 220, and 230°C). Compression molding (Dr. Collin press machine, Ebersberg, Germany) was used for producing sheets with required thickness from pelletized blends and nanocomposites. The molding performed in 240°C for all samples. All sample preparations and experiments were done immediately after drying for 4 h at 90°C because of the hydrophilic character of PA6 and Clay.

Table I. Designation and Composition of the Samples Introduced in this Work

Sample	HDPE	HDPE-*g*-Si	PA6	MMT
HDPE	100	0	0	0
Pen1	100	0	0	1
Pen2	100	0	0	4
PEs	0	100	0	0
PEsn	0	100	0	4
PA6	0	0	100	0
Pan	0	0	100	4
PEPA	100	0	20	0
PEPAn1	100	0	20	1
PEPAn2	100	0	20	4
PEPAs	0	100	20	0
PEPAsn1	0	100	20	1
PEPAsn2	0	100	20	4

CHARACTERIZATIONS

FTIR Studies

Fourier transfer infrared spectra were obtained using Equinox 55 instrument from Bruker Company (Ettlingen, Germany). HDPE-*g*-Si samples for spectroscopy analysis were purified from residual VTMS by dissolving in hot refluxing xylene for 6 h, precipitate into acetone and then drying under vacuum at 80°C for 6 h.[24]

X-ray Diffraction Analysis

The gallery height (d-spacing) of neat clay itself and the clay in nanocomposites were measured at room temperature in the transmission mode using a small angle X-ray scattering (SAXS, Hecus, S3-Micro, Graz, Austria) with Cu Kα radiation of

wavelength of 1.542 A° operated at 50 kV and 1 mA, and scanning rate of 0.5°/min. The sample to detector distance was 263 mm. The test specimens were cut from compressed molding sheets with thickness of 1 mm, and the d-spacing of organoclay was computed by applying the Bragg's equation:

$$2d \sin \Theta = n\lambda$$

where the variable d is the distance between clay layers, Θ and λ are the certain angles and wavelength of incidence, respectively, and n is an integer.

SEM Study

A scanning electron microscope VEGA (TESCAN, Brno, Czech Republic) operating at an accelerating voltage of 20 kV was used to inspect the phase morphology. Samples (cut from 2-mm-thickness sheet) were carefully broken at liquid nitrogen atmosphere; the fractured surfaces were then etched out by immersion in formic acid for 14 h at room temperature to remove the minor PA6 phases to emphasize the contrast between phases. The prepared surface was finally coated with a thin layer of gold to avoid electrostatic charging during examination.

TEM Analysis

The transmission electron microscope images were obtained by a FEI/Philips EM 208S microscope (Eindhoven, The Netherlands) operating at accelerating voltage of 100 kV for indicating the location of clay particles and intercalation of each polymer molecules in the clay galleries. The nanocomposite samples were cut with an ultramicrotome to observe the particles on their edges. Ultramicrotomed slices of 30 nm thick cut with diamond knife were finally mounted on a copper grid.

Rheological Characterization

Dynamic rheological characterizations were carried out on Rheoplus, MCR-300 rheometer (Anton Paar, Graz, Austria) in oscillatory mode at 5% strain (in linear viscoelastic region) using the 25 mm parallel plate fixture, with a gap of 1 mm at 240°C, under nitrogen blanket. The samples used in this study were fabricated in a disk with 1 mm in thickness by compression molding. The frequency sweeps from 0.01 to 600 rad/s.

Permeability Measurements

The oxygen permeation rate of samples was determined using a gas permeability tester (Brugger, GPD-C, Munich, Germany). The results were recorded as a volume of oxygen permeated from the films on the basis of pressure difference in two chambers in specified time. The test specimens were produced by Haake Rheomix Cast film (Thermo Scientific, Germany) with thickness of about 180 μ. These films were cut into circles 15 cm in diameter. The permeation test was carried out in ambient temperature and 35% relative humidity.

Immersion and evaporation were used for calculating the hydrocarbon permeability and solubility.[6,14] Samples were immersed in cyclohexane and thermostated at 50°C for 24 h. The solubility values were calculated from weight gain after surface drying. These specimens then placed at 70°C for 24 h and permeation rate calculated from weight of solvent evaporated.

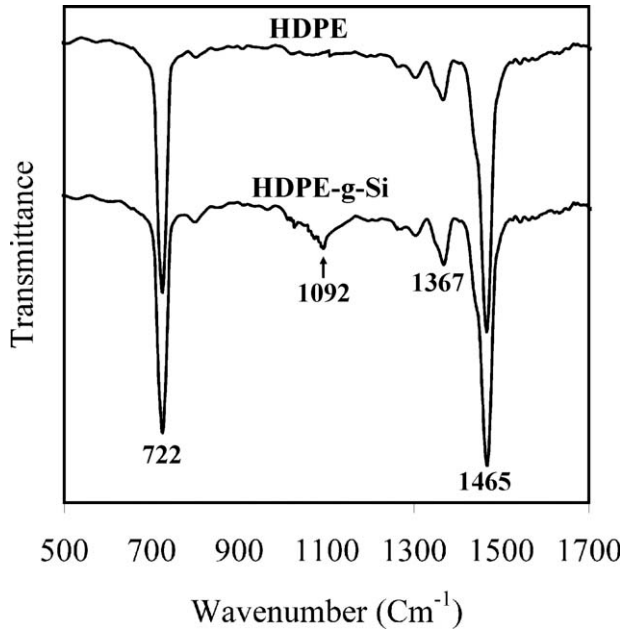

Figure 1. FTIR spectra of neat HDPE and HDPE-*g*-Si, indicating a peak around 1092 which shows Si-OCH_3 groups.

RESULTS AND DISCUSIONS

Grafting of VTMS on PE

In studying FTIR spectra, the transmittance peaks of interest which shows the trimethoxysilane groups (Si-OCH_3) are located in 799, 1092, and 1192 cm^{-1} wavenumbers.[28–30] The 1092 cm^{-1} is used as an indication of silane grafting extension in samples of this study, which typically has the strongest absorbance compared to other peaks.[31] Figure 1 shows the transmittance peaks of the HDPE in comparison with this polymer after grafting reaction. Obviously, the neat PE has no peak at mentioned wavenumbers. Therefore, the peak around 1092 cm^{-1} in grafted samples corresponds to the stretching vibration of Si-OCH_3 groups and demonstrate successful grafting reaction on HDPE molecules.

Because CH bending of methyl groups (the peak around 1367 cm^{-1}) are remained almost unchanged during silane grafting reaction and CH_2 bonds of PE (the peak around 722 cm^{-1}) are the branch point in this process, the absorbance ratio of transmittance peak of Si-OCH_3 to CH_2 or CH is usually used to quantitative normalization of grafting efficiency.[30] The absorbance ratio of 1092 to 722 peaks of our samples in this study is about 19.5%.

Investigation of Clay Dispersion in Nanocomposites

The principle of polymer/clay nanocomposite is based on increasing the gallery space of nanoclay due to insertion of polymer chains between clay layers; thus, X-ray analysis was addressed first to determining the effect of nanocomposite matrix on delamination of clay layers.

The SAXS profiles of Cloisite® 15A along with the angular dependences of the scattering intensities of various nanocomposites based on individual polymer matrices are shown in Figure 2. The pristine clay (curve a) showed the characteristic peak at

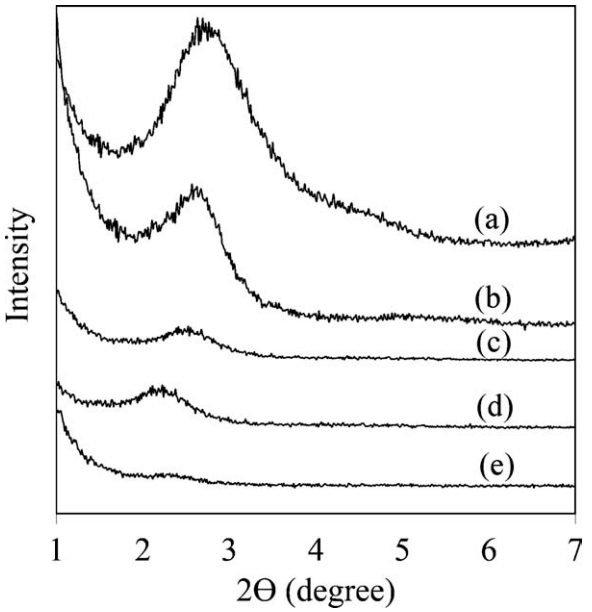

Figure 2. SAXS patterns of (a) Closite® 15A and various nanocomposites: (b) PEn2, (c) PEn1, (d) PEsn, and (e) Pan.

a 2Θ of around 2.8 corresponding to the d-spacing of 30.35 A° according to Bragg equation ($2d \sin \Theta = n\lambda$). As it could be seen obviously, the position of characteristic peak of nanocomposites based on neat HDPE (curve b and c) did not change significantly, and thus, nongrafted PE chains did not intercalate efficiently into the clay galleries. The curve c also indicated that SAXS analysis was able to show basal reflection of clay in low concentrations. On the other hand, the basal reflection for the clay was shifted to lower angle in the curve d (nanocomposite with HDPE-*g*-Si as matrix) which implied a higher d-spacing ($d = 38.4$ A°), indicating the intercalation of polymer chains inside the clay galleries. Furthermore, the intensity of the diffraction peak d was decreased significantly, which corresponded to lower concentration of the clay with mentioned d-spacing in related nanocomposites.[32,33] Thus, we can conclude that some part of Cloisite® 15A was successfully delaminated in the grafted PE. This agrees with what we reported in our previous paper in which the compatibilization effect of silane grafting for HDPE/Cloisite® 15A systems was demonstrated by combining several analyses.[22] Finally, absence of any characteristic peak of the organoclay in the PAn nanocomposite (curve e) at examined 2Θ values indicated that the Org-MMT plates were completely delaminated by PA6 chains because of their hydrophilic nature, consistent with previous results.[16,19,20]

Figure 3 shows the diffraction spectra for the nanocomposites prepared by PEPA and PEPAs blends as matrices in comparison with pristine PEPA blend. As it was expected, blend without organoclay (curve e) did not exhibit any characteristic peak at examined 2Θ values. HDPE/PA6/clay nanocomposite with 4 phr clay (PEPAn2) showed a relatively weak basal reflection at the same angular position with the HDPE/clay composites (curve b and c of Figure 2). This suggests that not only most of nanoparticles were delaminated in the PA6 but also small amount of clay were located in PE phase of the blend. Contrarily, basal reflection was disappeared when only 1 phr organoclay incorporated in the blend (PEPAn1). We believe that all of the clay was located in the PA6 phase (the validity of these assumptions confirmed by TEM observation). And finally, imperceptible spectra observed for the PEPAsn2 (curve d) was attributed to high affinity of organoclay to both PA6 and HDPE-*g*-Si polymers. Thus, organoclay was dispersed and delaminated in both PA6 and grafted PE phases. The similar observation was reported by Mallick et al. for using maleic compatibilizer in PE/PA6/clay systems.[20]

As X-ray diffraction alone is not enough to define the location of the clay plates in the blend nanocomposites, TEM micrograph is used to directly visualize the dispersion state of clay layers. Figure 4 represents the TEM images of PEPAn1, PEPAn2, and PEPAsn2 nanocomposites. The black lines and regions generally represent the clay layers cross-sections and background represents the polymeric matrix. The TEM images of Figure 4(a) revealed that in the PEPAn1 nanocomposite, because of difference in affinity of organoclay toward polymers along with low amount of clay in formulation, the clay platelets were tended to disperse and locate mostly inside the PA6 phase not in the HDPE matrix. The TEM image of the PEPAn2 composite in agreement with SAXS analysis showed that some portion of organoclay were located in the matrix without any intercalation and orientation of clay particle.

Figure 4(c–e) shows the TEM images of the PEPAsn2 nanocomposite in different magnifications. In the image with low magnification [Figure 4(c)], PA6 phase appeared as darker droplet regions due to the presence of clay in it. On the other hand, Figure 4(d) indicated that in this sample, clay layers not only located in minor phase but also nicely delaminated by HDPE-*g*-Si matrix. Finally, Figure 4(e) focused on interface area of two phases in the PEPAsn2 nanocomposite in which considerable presence of delaminated structure of nanoclay layers was obtained. These observations are in agreement with SAXS

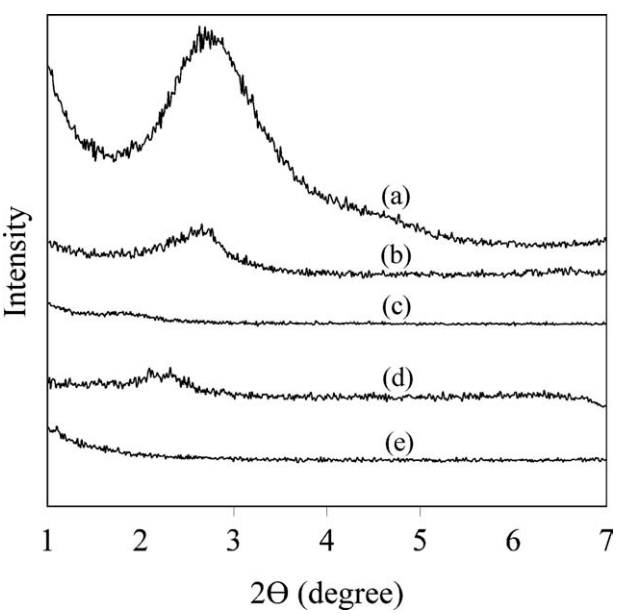

Figure 3. SAXS patterns of (a) Closite® 15A, (b) PEPAn2, (c) PEPAn1, (d) PEPAsn2, and (e) PEPA blend.

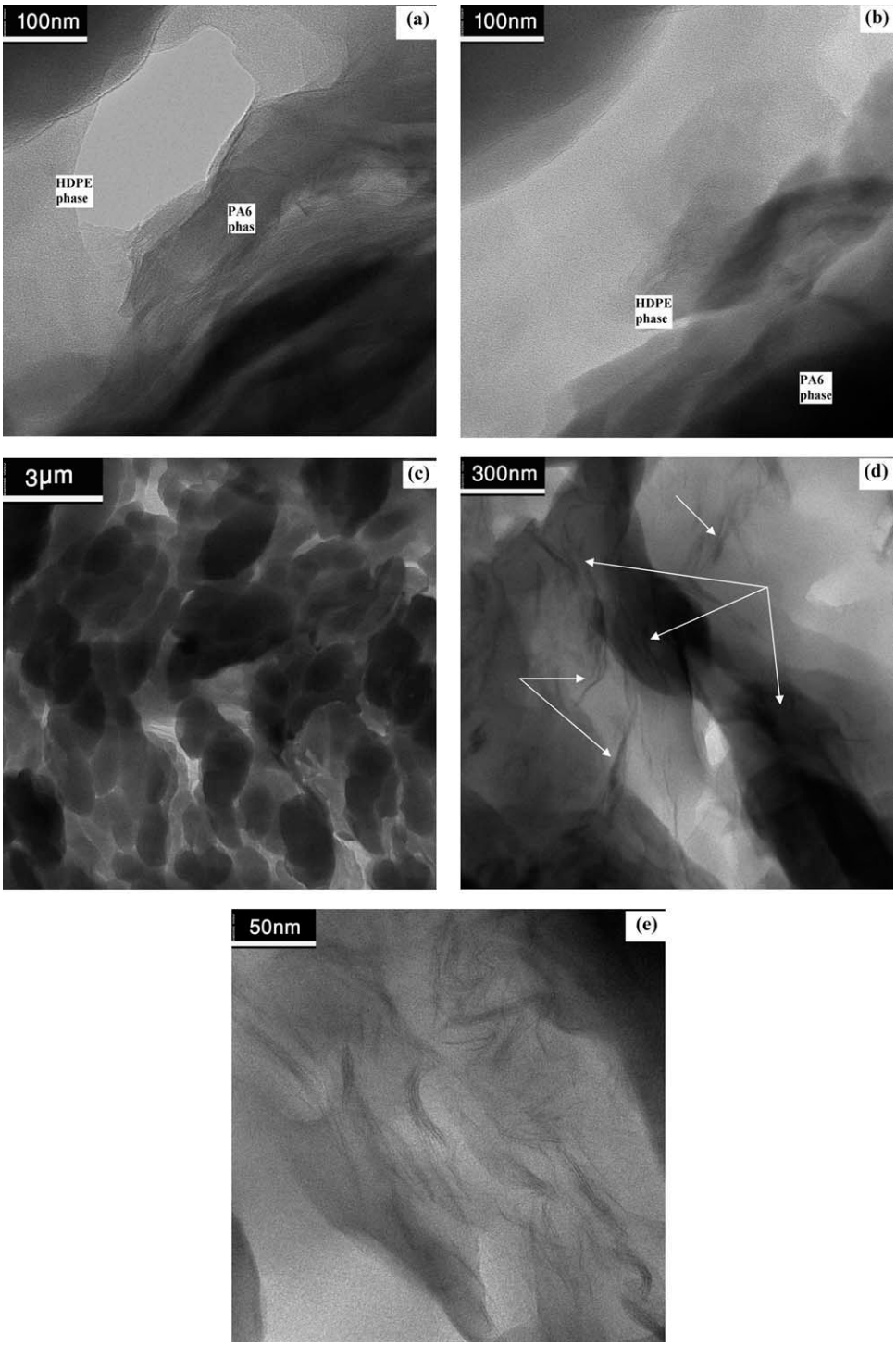

Figure 4. TEM images of: (a) PEPAn1, (b) PEPAn2, and (c,d,e) PEPAsn2 nanocomposites.

analysis and confirmed that silane grafting mediates the polarity between HDPE and Cloisite® 15A and had a significant effect on compatibilization of HDPE and organoclay.

Rheological Characterization

Rheological studies provide an appropriate investigation tool to consider the effect of melt state behavior on blend properties and morphology. Therefore, dynamic frequency tests were conducted in linear viscoelastic region (strain = 5%) to determine complex viscosity (η^*), and storage modulus (G') of the samples as a function of angular frequency (ω), as well as study on microstructure of blends.

Viscosity and G' of neat polymers along with their nanocomposites are compared in Figure 5 (a) and (b), respectively. As shown from results in Figure 5(a), HDPE and its

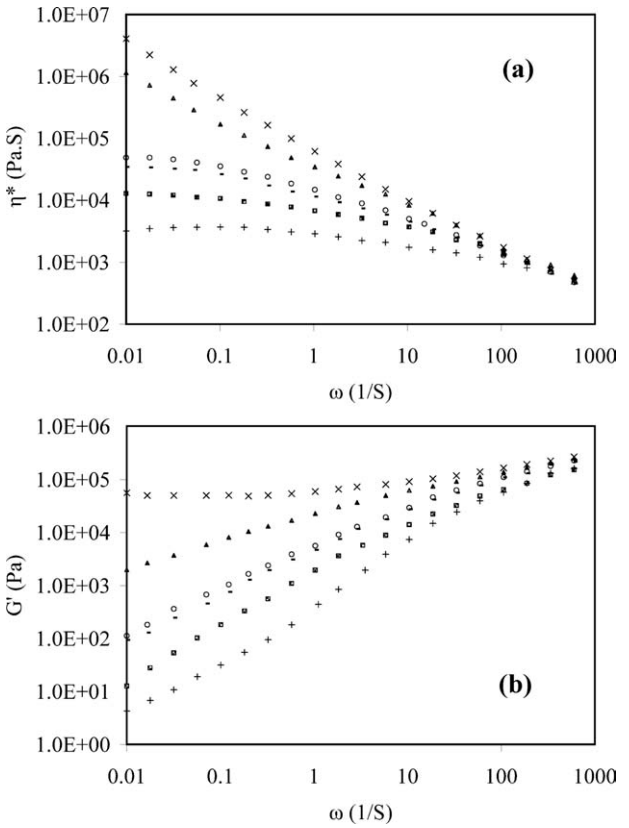

Figure 5. (a) Complex viscosity and (b) storage modulus of the neat polymers and their nanocomposites as a function of frequency: (▬) HDPE; (○) PEn2; (▲) PEs; (×) PEsn; (+) PA6; and (■) Pan.

nanocomposite showed a Newtonian plateau in η^*-ω curve at low frequency regions, whereas silane-grafted HDPE and PEsn samples showed shear thinning behavior in all frequency ranges. The viscosity also increased noticeably with the grafting of HDPE at low frequencies which is ordinary for silane-grafted PE.[22,27]

Moreover, the increase in η^* with incorporation of nanoclay into the grafted matrix was more considerable than that in HDPE. These results confirmed increased interactions between nanoclay and HDPE-*g*-Si polymer, which reduced chain mobility and flowability of nanocomposite. On the other hand, addition of 4 phr clay increased the viscosity of PA6 in all ω regions significantly, while the Newtonian behavior at low frequencies was remained unchanged. These findings were evident of mobility hindrance of PA chains because of high interactions between clay and PA6.[17]

Figure 5(b) shows that in neat PE, PA6, and their nanocomposites, G' increased monotonically by increasing frequency. This was attributed to typical behavior of a viscoelastic liquid. In spite of PEn2, relatively considerable increase in the elasticity (at lower ω regions) was observed with addition of organoclay to PA6 (PAn sample). The similar observation was reported by Filippone et al.[18] These results imply that there was significant interactions between the clay layers and PA6 chains; however, the small increase occurred in G' of PEn2 could be just defined as a filler effect.

A significant increase in storage modulus of HDPE-*g*-Si attributed to the structural change of PE. The elasticity of the PEsn nanocomposite was also the highest in the entire range of frequency studied. Furthermore, it was observed that at lower frequencies, G' exhibited diminished frequency dependence for this nanocomposite which is the characteristic behavior of solid-like materials. These behaviors of G' were evident of physical network formation between the clay layers and polymer chains.[10]

The rheological properties of the blends and their nanocomposites with two levels of organoclay are illustrated in Figure 6. The unfilled 80/20 HDPE/PA6 blend (PEPA sample) exhibited the Newtonian plateau in η^*-ω curve, relatively similar to their components. The viscosity of blend also not changed appreciably from viscosity of HDPE matrix over the entire frequency range [see Figure 5(a) and 6(a)]. These observations indicated poor interfacial adhesion between two phases, and have been reported for LDPE/PA systems as well.[15] Moreover, not only G' of this blend showed viscoelastic liquid behavior but also a relaxation shoulder was created at frequencies around 0.3 s^{-1} [Figure 6(b)] due to shape relaxation of dispersed phase. This behavior reflects typical characteristics of incompatible, biphasic polymer blends with droplet morphology.[34] On the contrary, blend of HDPE-*g*-Si and PA6 interestingly exhibited the

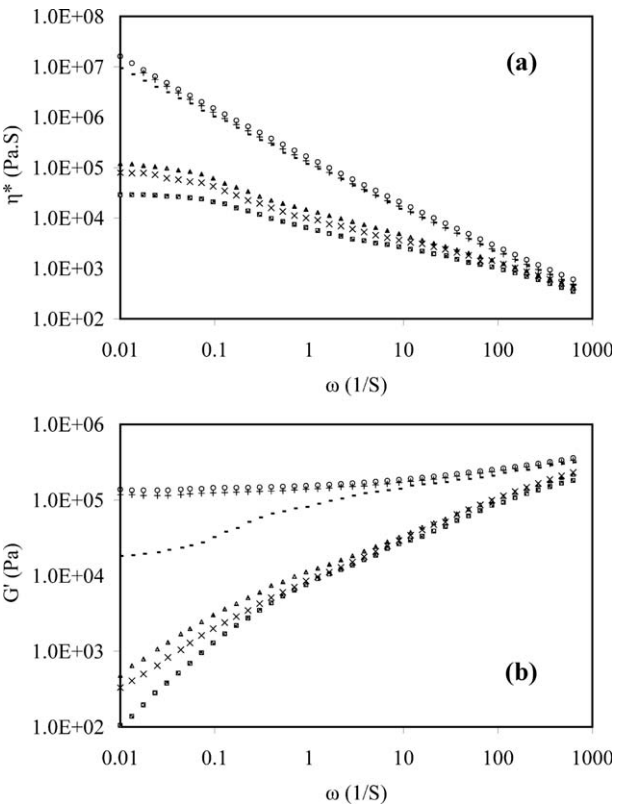

Figure 6. (a) Complex viscosity, and (b) storage modulus of the blends as a function of frequency: (▬) PEPAs; (+) PEPAsn1; (○) PEPAsn2; (■) PEPA; (×) PEPAn1; and (▲) PEPAn2.

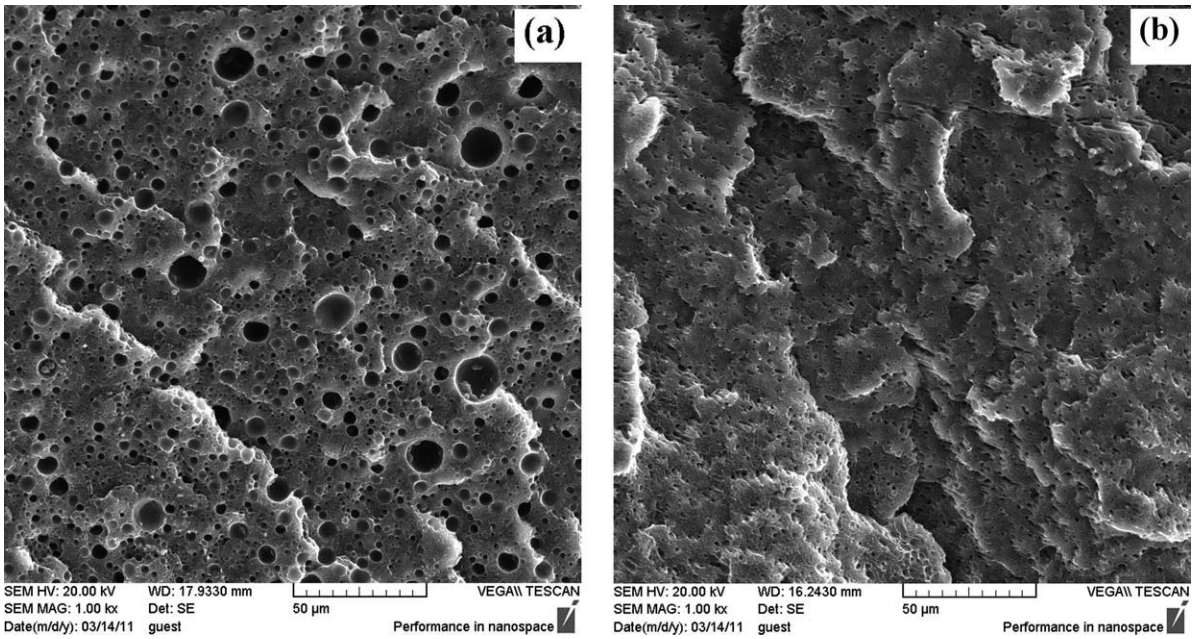

Figure 7. SEM images of etched (a) PEPA and (b) PEPAs blends.

rheological behavior of compatibilized blends. The comparison between Figures 5 and 6 showed η^* and G' of PEPAs blend were remarkably exceeded the value of their constituents over all frequencies. In addition, a secondary plateau modulus was observed in elasticity curve at terminal region. A valid explanation for the enhanced elasticity and viscosity of blend and also solidlike behavior of blend in low frequencies is creation of compatibilized blend, which arises from increased interaction between phases.[17,34–36] Here, this effect could be applied by polar–polar interactions between the amide groups of PA6 and methoxy silane groups of the HDPE-*g*-Si.

Besides, organoclay has a substantial effect on the viscoelasticity of the PEPA blend. As observed from Figure 6, the viscosity and elasticity were increased by about 5e+4 pa.s and 230 pa, respectively, after addition of 1 phr organoclay to the PEPA. The further increase was also obtained by increasing amount of clay to 4 phr; however, the overall trends and relaxation shoulder of all blends remained unchanged. Therefore, these enhancements could just be ascribed to changes in viscoelastic behavior of constituents (see Figure 5), as well as possibility of suppressing interfacial slip, due to localization of the clay particles in the interface area of the blend.[15–21]

Although, the interfacial adhesion is fairly high in the PEPAs blend, further improvement in η^* and elasticity were obtained by incorporation of nanoclay. In addition, G' of PEPAsn1 and PEPAsn2 nanocomposites showed solidlike behavior in low frequencies. The existence of three-dimensional physical network or even co-continuous blend morphology was generally proposed to explain the solidlike feature of polymeric blends.[17,36] These rheological behaviors arise from higher clay attraction to grafted PE which caused more variation of matrix phase viscoelasticity and also greater adhesion between phases by dispersing clay in the interface.

SEM Studies

The SEM micrographs are used to investigate the changes of phase morphology of HDPE/PA blends at fixed composition (100/20) as function of silane grafting of PE and/or incorporating nanoclay, and the results are shown in Figures 7 and 8. The blend of neat HDPE with PA6 without clay [Figure 7(a)] exhibited a globular microstructure and clearly demonstrated biphasic matrix-droplet morphology. The minor phase (PA6) dispersed as large spherical domains in HDPE matrix which attributed to the high interfacial tension between two polymeric phases. In a blend, the morphology of the dispersed phase results from a delicate balance between shear forces, which tend to deform the droplets, and interfacial tension, which tend to resist to the droplet deformation. Therefore, because of the high interfacial tension between immiscible polymers, the spherical morphology is the most thermodynamically favored because leads to the minimization of the specific interfacial area.[17,19,37]

On the other hand, the substantial reduction in dispersed phase size morphology is obtained by silane grafting of PE matrix [Figure 7(b)]. Decrease in domain sizes is an evidence of improvements in interfacial adhesion between phases and increase of matrix viscosity by silane grafting[37] [see Figure 5(a)]. Similar observations were also proposed for using different compatibilizers in PE/PA systems.[9,13,20] Furthermore, the nonspherical shape of the voids of the removal PA particles indicated that the interfacial tension between HDPE-*g*-Si and PA6 phases is relatively low. As demonstrated previously, these explanations confirmed this fact that modification of HDPE by silane grafting mediates polarity between HDPE and PA6 and has a strong effect on compatibilization of their blends.

SEM micrographs in Figure 8 represent the effect of organoclay on morphology of the blends. Comparison of nodule sizes in Figures 7(a) and 8(a) reveals that when a small amount of clay

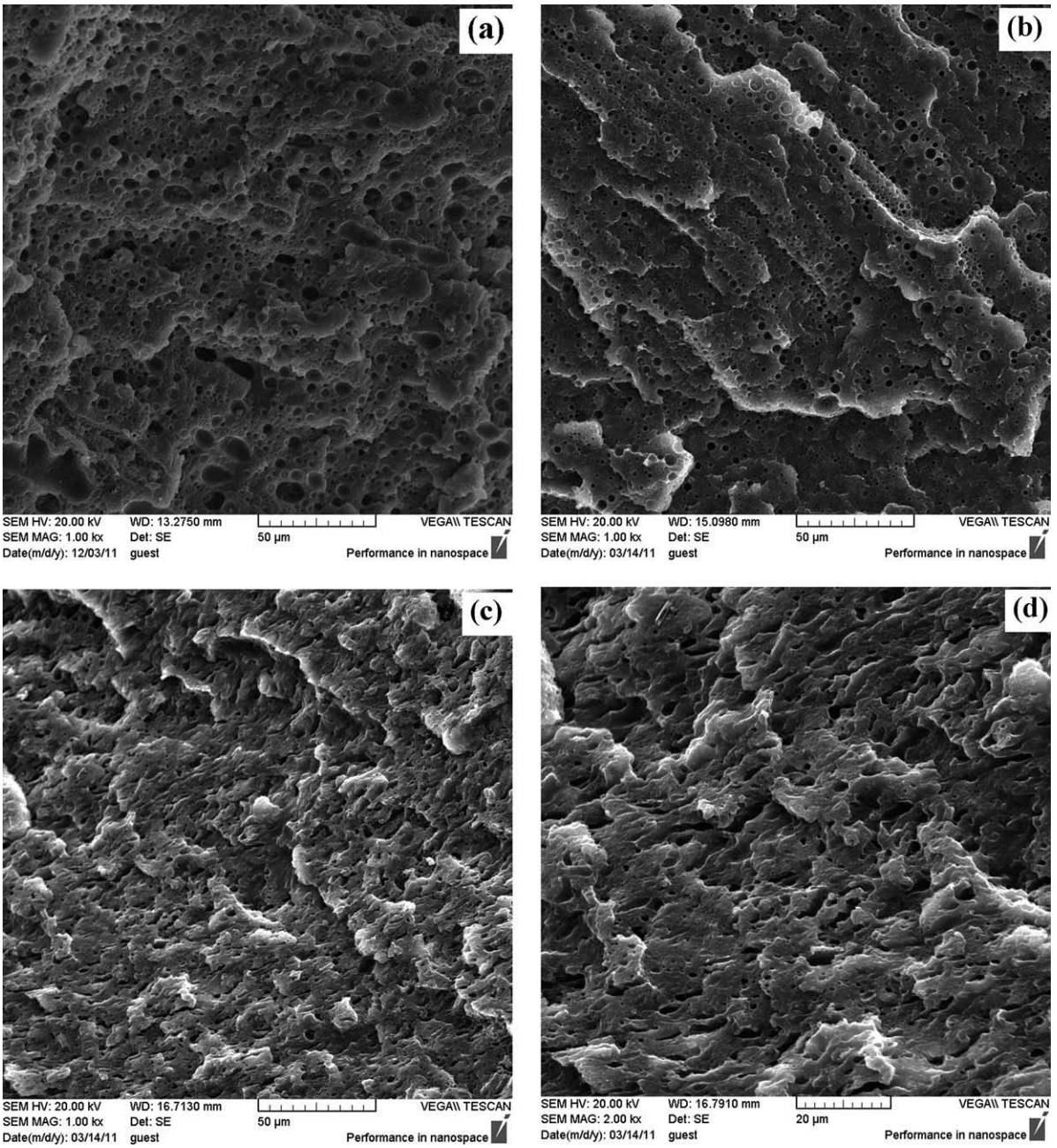

Figure 8. SEM images of (a) PEPAn1, (b) PEPAn2, and (c,d) PEPAsn2 nanocomposites.

(1 phr) was used, dispersed domain size of the PA6 phase was reduced slightly. In addition, much more significant difference in the domain sizes and more narrow size distribution are observed by increasing amount of clay to 4 phr [Figure 8(b)]. This indicates that the organoclay played a drastic role in decreasing the dispersed phase sizes of PEPA blends. However, the micro voids surrounding the PA6 droplets and their spherical shape indicate that the interfacial adhesion is still weak.

Because increase of minor phase viscosity and elasticity due to location of clay into it has a reverse effect on dispersed size[37]; and all of 1 phr clay was mostly dispersed in the PA6 phase, as evident from SAXS and TEM studies [Figures 3 and 4(a)]; possible explanation for small reduction of domain size in this case is change in viscosity ratio of blend constituents.

X-ray and TEM studies (see Figure 3) suggested that in nanocomposite based on HDPE and PA6 with 4 phr clay (PEPAn2), nanoparticles either exfoliated in the PA6 phase, or located in the PE phase of the blend. Thus, further size reduction and uniformity observed in nodules could be attributed to this fact that nanoclay dispersed in PE matrix acted as nucleating agent for promoting initiation of the dispersed phase separation during melt-blending of two polymers. This effect resulted in formation of lots of PA6 nucleation sites. Furthermore, because the clay resides in the PE phase in microscale and no intercalation was

occurred, the clay particles cannot effectively act as a barrier to delay and minimize droplets coalescence.

Finally, Figure 8(c,d) shows the blend morphology in presence of organoclay along with silane grafting of PE matrix in two magnifications. Interestingly, extremely fine and elongated microstructure was obtained for the PEPAsn2 blend. The feasible theories for describing the further size reduction are: (i) improvement of matrix viscosity and elasticity, as described above in rheological characterization (see Figure 5). These parameters caused increase in shear forces during melt compounding[37]; (ii) silane grafting of PE make it compatible with both PA6 and the organoclay because of hydrophilic characteristic of silanol groups. Thus, dispersed clay in the interface has higher affinity to both phases and consequently further increase in interfacial adhesion was achieved; (iii) some part of the organoclay was delaminated in the HDPE-*g*-Si phase (see also results of SAXS and TEM) and the clay layers serve as barrier which suppressed the coalescence and the agglomeration of the dispersed phase.[18–20,38]

However, the observed unexpected occurrence of elongated shape of dispersed phase cannot be simply explained in terms of changes in viscosity of the blend constituents.[39,40] Filippone et al. comprehensively discussed this phenomenon for HDPE/PA6/nanoclay systems.[18] Their results showed that when PA6 is the minor phase, a percolating network forms above critical filler to PA ratio (clay/PA6 about 0.2, same to our sample), in which the PA gets continuous as it coats a space across organoclay network. Besides, elevated viscosity of the filled PA6 and interaction between phases prevented the break-up of elongated droplets during melt compounding.

Permeability Measurements

In the case of PE/PA blends and their nanocomposites, an improvement of barrier property is one of the most fundamental consequences because of their applications. The oxygen permeation rates (Po_2) along with hydrocarbon barrier property of our samples are presented in Table II. Po_2 in this chart presented in cm^3 of oxygen permeate per square meter of sheet surface in one day (cm^3/day m^2 bar). As mentioned above in characterization section, hydrocarbon barrierity was measured based on weight measurements, after immersion of the samples in the cyclohexane (a nonpolar hydrocarbon known as a high permeable in polyolefins) at 50°C for 24 h, followed by put them in the evaporation conditions.[6] Consequently, penetration amount of cyclohexane (S) was measured on the basis of the samples weight gain (%), and cyclohexane permeation rate (Pc) was estimated on the basis of weight of cyclohexane evaporated at 70°C per square meter of sheet surface in one day (g/day m^2).

The results show that presence of organoclay and PA generally reduced the permeability of samples; however, PA6 was more effective on barrier efficiency against cyclohexane than oxygen. Interestingly, the silane-grafted specimens showed the worst barrier properties of these samples, so that oxygen and cyclohexane permeates from grafted PE about 1.7% and 0.8%, respectively, more than neat HDPE. Because it is generally recognized that permeant molecules can only permeates through noncrystalline regions, this effect attributed to increasing of amorphous region by grafting of PE chains. Effect of silane grafting on crystallization behaviour of PE was investigated in our previous work.[22]

Table II. Oxygen Permeability (Po_2), Cyclohexane Penetration (*S*), and Cyclohexane Permeability (Pc) of the Samples

Sample	Po_2 (cm^3/day m^2 bar)	*S* (% w/w)	Pc (g/day m^2)
HDPE	408	18.0	108.2
Pen	379	17.7	102.0
PEs	415	18.9	109.1
PEsn	246	15.1	84.2
PA6	302	1.66	18.2
PAn	244	1.24	12.8
PEPA	382	14.7	89.8
PEPAn1	328	14.0	71.4
PEPAn2	317	13.5	65.0
PEPAs	291	10.2	63.3
PEPAsn1	216	9.3	51.2
PEPAsn2	201	8.8	40.4

In agreement with our prediction, silane grafting of PE enhanced barrierity of both PE/PA blends and PE nanocomposites. The permeation rate of oxygen and cyclohexane reduced by 23.8% and 29.5% for PEPAs, and 35.1% and 17.4% for PEsn, compared with PEPA and PEn2 specimens, respectively. This improvement demonstrated compatibilization effect of silane grafting, so that finer PA6 dispersion or better delamination of the clay particles is obtained, which creates more tortuous path for the diffusion in amorphous regions. Furthermore, unlike nanocomposites based on neat PE matrix which showed a small enhancement in the barrierity, incorporating nanoclay in the PE/PA systems showed a considerable effect on barrierity of samples. This improvement arises from increased barrier efficiency of dispersed phase by exfoliation of clay into the PA6 and reduced size of minor phase (see Table II and Figure 8).

Finally, we can see that nanocomposites based on blend of HDPE-*g*-Si and PA6 as a matrix (PEPAsn1 and PEPAsn2) exhibited excellent permeation resistant to both cyclohexane and oxygen. The permeation rates of specimens prepared in this study reach the minimum of Po_2 = 201 cm^3/day m^2 bar and Pc = 40.4 g/day m^2 for the PEPAsn2 specimen, which are more than 100% smaller than PE sample. These indications explained by synergetic effect of silane grafting and organoclay for producing the finest and elongated morphology, along with dispersion and delamination of clay particles in more permeable PE phase.

CONCLUSIONS

This study focused on the effect of incorporating organocaly and silane grafting of HDPE on morphological, rheological, and barrier properties of HDPE/PA6/clay ternary nanocomposites prepared via melt blending in corotating twin-screw extruder. It was shown that silane grafting not only compatibilized HDPE with PA6 but also increased interactions between PE and organoclay led to delamination of the clay layers in the matrix. It was also demonstrated that the resulting rheological and barrier properties were sensitive to blend morphology.

SAXS and TEM study indicated that unlike nanocomposites based on blend of HDPE and PA6, which most of organoclay

were exfoliated in the minor phase, clay particles were dispersed in both PA6 and grafted PE matrix phases.

The noticeable interaction between organoclay and PA6 as well as increased interactions of nanoclay and silane-grafted PE were confirmed by rheological results. In spite of poor interfacial adhesion in the PEPA sample, blend of HDPE-*g*-Si and PA6 exhibited the rheological behavior of compatibilized systems. Nevertheless, these observations showed that organoclay had a substantial effect on the viscoelasticity of the PE/PA systems.

Most observations of the morphological study highlighted the significant role of silane grafting as well as presence of organoclay on size and shape of dispersed phase. This could be concluded that both these modifications played a significant role on morphology of the HDPE/PA6 blends, where nanoclay acted as a nucleating agent and/or barrier to coalescence of PA6 droplets and silane grafting along with location of clay in interface mediated the polarity between two phases and caused improved interfacial adhesion.

Furthermore, we can see from this study that the morphology and not only the blend composition have to be considered to evolution of barrier properties. It was demonstrated that, presence of organoclay and/or PA6 generally reduced the permeability of the samples. Besides, silane grafting of PE enhanced barrierity of both PE/PA blends and PE nanocomposites because of its compatibilizing effect, which caused finer blend morphology or more delaminated clay in the nanocomposites. Finally, nanocomposites based on HDPE-*g*-Si/PA6 blend as a matrix exhibited excellent permeation resistant to both cyclohexane and oxygen.

At the end, we can conclude that silane grafting is an economical and easily accessible method for compatibilization of HDPE and PA6, which in addition to modification of rheological behavior and morphology of blends has an advantage of increasing interactions between PE and nanoclay.

REFERENCES

1. Choudalakis, G.; Gotsis, A. D. *Eur. Polym. J.* **2009,** *45*, 967.
2. Lange, J.; Wyser, Y. *Packag. Technol. Sci.* **2003,** *16*, 149.
3. Jacquelot, E.; Espuche, E.; Gerard J. F.; Duchet, J.; Mazabraud, P. *J. Polym. Sci. Part B: Polym Phys.* **2006,** *44*, 431.
4. Yeh, J. T.; Fan-Chiang, C. C.; Yang, S. S. *J. Appl. Polym. Sci.* **1997,** *64*, 1531.
5. Lee, S. Y.; Kim, S. C. *Polym. Eng. Sci.* **1997,** *37*, 463.
6. Erdmann, E.; Acosta, D.; Pita, V. J. R. R.; Monasterio, F. E.; Carrera, M. C.; Dias, M. L.; Destefanis, H. A. *J. Appl. Polym. Sci.* **2010,** *118*, 2467.
7. Yeh, J. T.; Jyan, C. F.; Yang, S. S.; Chou, S. *Polym. Eng. Sci.* **1999,** *39*, 1952.
8. Kamal, M. R.; Garmabi, H.; Hozhabr, S.; Arghyris, L. *Polym. Eng. Sci.* **1995,** *35*, 41.
9. Filippi, S.; Chiono, V.; Polacco, G.; Paci, M.; Minkova, L. I.; Magagnini, P. *Macromol. Chem. Phys.* **2002,** *203*, 1512.
10. Durmus, A.; Maybelle, W.; Kasgoz, A.; Macosko, C. W.; Tsapatsis, M. *Eur. Polym. J.* **2007,** *43*, 3737.
11. Ranade, A.; Nayak, K.; Fairbrother, D.; D'souza, N. A. *Polymer* **2005.** *46*, 7323.
12. Qian, Z.; Zhou, Hu.; Xu, X.; Ding, Y.; Zhang, Sh.; Yang, M. *Polym. Compos.* **2009,** *30*, 1234.
13. Chatreenuwat, B.; Nithitanakul, M.; Grady, B. P. *J. Appl. Polym. Sci.* **2007,** *103*, 3871.
14. Wang, Q.; Qi, R.; Shen, Y.; Lio, Q.; Zhou, Ch. *J. Appl. Polym. Sci.* **2007,** *106*, 3220.
15. Filippi, S.; Dintcheva, N. T.; Scaffaro, R.; La Manita, F. P.; Polacco, G.; Magagnini, P. *Polym. Eng. Sci.* **2009,** *49*, 1187.
16. Fang, Zh.; Xu, Y.; Tong, L. *Polym. Eng. Sci.* **2007,** *47*, 551.
17. Filippone, G.; Dintcheva, N.Tz.; Acierno, D.; La Mantia, F. P. *Polymer* **2008,** *49*, 1312.
18. Filippone, G.; Dintcheva, N.Tz.; La Mantia, F. P.; Acierno, D. *Polymer* **2010,** *51*, 3956.
19. Mallick, S.; Khatua, B. B. *J. Appl. Polym. Sci.* **2011,** *121*, 359.
20. Mallick, S.; Kar, P.; Khatua, B. B. *J. Appl. Polym. Sci.* **2012,** *123*, 1801.
21. Mehrabzadeh, M.; Kamal, M. R. *Polym. Eng. Sci.* **2004,** *44*, 1152.
22. Sharif-Pakdaman, A.; Morshedian, J.; Jahani, Y. *J. Appl. Polym. Sci.* **2012,** *125*, E305.
23. Wang, H.; Fang, P.; Chen, Z.; Wang, Sh.; Xu, Y.; Fang, Zh. *Polym. Int.* **2008,** *57*, 50.
24. Lu, H.; Hu, Y.; Li, M.; Chen, Z.; Fan, W. *Compos. Sci. Technol.* **2006,** *66*, 3035.
25. Nachtigall, S. M. B.; Felix, A. H. O.; Mauler, R. S. *J. Appl. Polym. Sci.* **2003,** *88*, 2492.
26. Shim, J. H.; Joo, J. H.; Jung S. H. *J. Polym. Sci. Part B: Polym. Phys.* **2007,** *45*, 607.
27. Morshedian, J.; Mohammad-hoseinpour, P. *Iran. Polym. J.* **2009,** *18*, 103.
28. Mallegol, J.; Carlsson, D. J.; Deschenes, L. *Polym. Degrad. Stab.* **2001,** *73*, 259.
29. Hjertberg, T.; Palmlof, M.; Sultan, B. A. *J. Appl. Polym. Sci.* **1991,** *42*, 1185.
30. Sirisinha, K.; Boonkongkaef, M.; Kositchaiyong, S. *Polym. Test.* **2010,** *29*, 958.
31. Morshedian, J.; Mohammad-hoseinpour, P.; Azizi, H.; Parvizzad, R. *EXPRESS Polym. Lett.* **2009,** *3*, 105.
32. Chu, D.; Nguyen, Q.; Baird, D. G. *Polym Compos.* **2007,** *28*, 499.
33. Shang, C.; Thompson, M. L. *Clay Clay Miner.* **1995,** *43*, 128.
34. Graebling, D.; Muller, R.; Palierne, J. F. *Macromolecules* **1993,** *26*, 320.
35. Sailer, C.; Handge, U. A. *Macromolecules* **2007,** *40*, 2019.
36. Jafari, S. H.; Potschke, P.; Stephan, M.; Warth, H.; Alberts, H. *Polymer* **2002,** *43*, 6985.
37. Utracki, L. A. Polymer Blends Handbook; Kluwer Academic Publishers: The Netherlands, **2002.**
38. Mederic, P.; Ville, J.; Huitric, J.; Moan, M.; Aubry, T. *Polym. Eng. Sci.* **2011,** *51*, 969.
39. Li, Y.; Shimizu, H. *Macromol. Rapid Commun.* **2005,** *26*, 710.
40. Ray, S. S.; Bandyopadhyay, J.; Bousmina, M. *Macromol. Mater. Eng.* **2007,** *292*, 729.